Lipids (2013) 48:307–318
DOI 10.1007/s11745-013-3760-z

METHODS

An Improved High-Throughput Lipid Extraction Method for the Analysis of Human Brain Lipids

Sarah K. Abbott · Andrew M. Jenner · Todd W. Mitchell · Simon H. J. Brown · Glenda M. Halliday · Brett Garner

Received: 16 August 2012 / Accepted: 24 December 2012 / Published online: 26 January 2013

Abstract We have developed a protocol suitable for high-throughput lipidomic analysis of human brain samples. The traditional Folch extraction (using chloroform and glass–glass homogenization) was compared to a high-throughput method combining methyl-*tert*-butyl ether (MTBE) extraction with mechanical homogenization utilizing ceramic beads. This high-throughput method significantly reduced sample handling time and increased efficiency compared to glass–glass homogenizing. Furthermore, replacing chloroform with MTBE is safer (less carcinogenic/toxic), with lipids dissolving in the upper phase, allowing for easier pipetting and the potential for automation (i.e., robotics). Both methods were applied to the analysis of human occipital cortex. Lipid species (including ceramides, sphingomyelins, choline glycerophospholipids, ethanolamine glycerophospholipids and phosphatidylserines) were analyzed via electrospray ionization mass spectrometry and sterol species were analyzed using gas chromatography mass spectrometry. No differences in lipid species composition were evident when the lipid extraction protocols were compared, indicating that MTBE extraction with mechanical bead homogenization provides an improved method for the lipidomic profiling of human brain tissue.

Keywords Lipidomics · Human-brain · Ceramide · Sphingomyelin · Phosphatidylcholine · Phosphatidylethanolamine · Phosphatidylserine · Sterol

Abbreviations

BHT	Butylated hydroxytoluene
BSTFA	(*N*,*O*-bis(trimethylsilyl)trifluoroacetamide
CE	Collision energy
Cer	Ceramide
CerPCho	Sphingomyelin
ChoGpl	Choline glycerophospholipid
CV	Coefficient of variation
CXP	Collision cell exit potential
DP	Declustering potential
EP	Entrance potential
ESI–MS	Electrospray ionization mass spectrometry
EtnGpl	Ethanolamine glycerophospholipid
GC-MS	Gas chromatography mass spectrometry
MTBE	Methyl-*tert*-butyl ether
MRM	Multiple reaction monitoring
NL	Neutral loss
PI	Precursor ion
PtdSer	Phosphatidylserine
SGalCer	Sulfatide
TMCS	Trimethylchlorosilane

S. K. Abbott · A. M. Jenner · T. W. Mitchell · S. H. J. Brown · B. Garner
Illawarra Health and Medical Research Institute, University of Wollongong, Wollongong, NSW 2522, Australia

S. K. Abbott (✉) · A. M. Jenner · B. Garner
School of Biological Sciences, University of Wollongong, Wollongong, NSW 2522, Australia
e-mail: sarahmac@uow.edu.au

T. W. Mitchell · S. H. J. Brown
School of Health Sciences, University of Wollongong, Wollongong, NSW 2522, Australia

G. M. Halliday
Neuroscience Research Australia and the University of New South Wales, Sydney, NSW 2031, Australia

Introduction

It is established that lipid metabolism changes profoundly during human brain development and ageing [1, 2]. There is also increasing evidence indicating that neurological disorders including Parkinson's disease [3, 4], Alzheimer's disease [5, 6], Huntington's disease [7] and Schizophrenia [8] are all associated with alterations in cerebral lipid homeostasis. In the case of Alzheimer's disease, three of the strongest genetic risk factors for the common late-onset form of the disease, i.e. *APOE, CLU, ABCA7*, are involved in brain lipid transport [9, 10]. This highlights the fact that altered brain lipid metabolism may not only be a consequence of the disease process but may in fact represent a causative factor that could be amenable to therapeutic targeting. There is clearly a great need to develop efficient methods that will facilitate the post-mortem analysis of human brain tissues by high-throughput lipidomic approaches. Such a method will help to clarify the extent to which altered lipid metabolism is associated with various human neurological conditions and may aid in the discovery of biomarkers for disease status as well as in monitoring treatment efficacy [11]. In the present study we aimed to develop an improved method that could provide an alternative for the widely used Folch extraction/glass–glass homogenization method.

Shotgun lipidomics involves the analysis of a crude lipid extract via electrospray ionization mass spectrometry (ESI–MS; see [12]). With recent advances in mass spectrometry, such as the employment of automated chip-based nanospray technology, the bottleneck for modern shotgun lipidomic studies is the time required for traditional lipid extraction. A typical lipid extraction usually follows the Folch extraction [13], which employs chloroform/methanol (2:1, by vol) and is generally accompanied by glass–glass homogenization. Although this method has become well-established over the last half century as one of the most popular lipid extraction techniques, there are some disadvantages, in terms of both safety and efficiency that need to be addressed. In particular, chloroform is highly toxic and carcinogenic. Previous lipid studies have solved this toxicity issue to some degree by replacing chloroform with dichloromethane (see [14, 15]). However, both these solvents are very dense, which is inconvenient during lipid extraction, as the lipids will dissolve in the lower chloroform layer during phase separation (i.e. difficult to pipette without contamination from the aqueous layer and also less compatible with the potential use of robotics). In addition to this, glass–glass homogenization is highly time-consuming and also increases the risk of cross-contamination between samples.

An alternative to traditional glass–glass homogenization is a new high-throughput technology that employs mechanical bead beater homogenization capable of homogenizing up to 96 samples within approximately 2 min. The risk of cross-contamination is also limited, as single-use disposable tubes containing ceramic beads are used for each sample. Variation between operators is also reduced as the mechanical bead homogenization is automated, making results more consistent and reproducible. Previous studies have processed normal and diseased human brain tissue for the measurement of fatty acid composition [16, 17], with bead homogenization results comparable to Potter–Elvehjem homogenization (equivalent to glass–glass). Other metabolomic studies have also employed automated bead homogenization for extraction and quantification of lipids (including glycerophospholipids and sphingolipids) from various tissue matrices, including mouse brain, kidney, liver, adipose tissue and muscle [18], as well as fish liver [19]. However, a direct comparison of the Folch glass–glass homogenization method with a mechanical bead homogenization has not been previously investigated.

A recent lipidomic study demonstrated that methyl-*tert*-butyl ether (MTBE) can effectively replace chloroform for the extraction of lipids from tissue matrices (including mouse brain, *Caenorhabditis elegans* eggs and *Escherichia coli*; see [20]). This MTBE extraction protocol has also been applied to measure lipids in cerebrospinal fluid of Alzheimer's disease patients [21, 22]. A Bligh and Dyer [23] variation of this MTBE protocol has also been utilized in previous lipidomic studies of human plasma [20, 24–26]. The main advantages of MTBE over chloroform are its lower toxicity and density (so that lipids dissolve in the upper layer during phase separation), which greatly improves safety and ease of sample processing (see [20] for more details).

To overcome the aforementioned problems associated with traditional lipid extraction techniques, protocol comparisons were made between the well-established Folch extraction (using glass–glass homogenization; i.e. "Glass-Chloroform") and a modified method that employed bead homogenization (Precellys®24) and, based on [20], replaced chloroform with MTBE (i.e. "Bead-MTBE"). The lipid composition of human occipital cortex was measured as a test sample. The lipid species measured by ESI-MS included: ceramides (Cer), sphingomyelins (CerPCho), choline glycerophospholipids (ChoGpl), ethanolamine glycerophospholipids (EtnGpl) and phosphatidylserines (PtdSer). In combination with this "shotgun" approach, the lipid extracts of human brain tissue were also subjected to a more targeted analysis of sterol species via gas chromatography mass spectrometry (GC–MS).

Materials and Methods

Materials and Internal Standards

MTBE, chloroform, methanol, acetone, hexane and acetonitrile were HPLC grade and purchased from Thermo Scientific, Scoresby, VIC, Australia; analytical grade butylated hydroxytoluene (BHT) and sodium hydroxide (98 % minimum) from Sigma Aldrich, Sydney, NSW, Australia; analytical grade ammonium acetate from Crown Scientific, Moorebank, NSW, Australia; 15 × 45 mm (4 mL) screw thread vials and 12 × 32 mm (1.8 mL) wide mouth vials (both with PTFE/silicone septa caps) from Grace Davison, Rowville, VIC, Australia. All solvents contained 0.01 % w/v BHT.

Two internal standard mixtures were added to each sample. Firstly, 4 μL/mg of tissue of the phospholipid/sphingolipid standard mixture containing: 75 μM CerP-Cho(d18:0/12:0), 75 μM Cer(d18:1/10:0), 500 μM PtdCho(19:0/19:0), 175 μM PtdSer(17:0/17:0), 225 μM PtdEtn(17:0/17:0), 25 μM Lyso PtdCho (17:0) and 25 μM Lyso PtdEtn (14:0) in chloroform/methanol (2:1, by vol); Avanti Polar Lipids purchased from Auspep, Tullamarine, VIC, Australia. Secondly, 10 μL/sample of sterols standard mixture in ethanol was added, including: desmosterol-d_6, 14-demethyl-lanosterol-d_6, (Avanti Polar Lipids), β-sitosterol-d_7, campesterol-d_3 and 7-ketocholesterol-d_7 (CDN Isotopes, Quebec, Canada) and 27-hydroxycholesterol-d_5 and 24-hydroxycholesterol-d_7 (Medical Isotopes, Inc, Pelham, AL, USA). Lanosterol, squalene, stigmasterol and 24,25-dihydrolanosterol were quantitated using other heavy sterol internal standards.

Human Brain Tissue

The human brain tissue was collected with written informed consent as approved by the Human Research Ethics Committee of the University of New South Wales (HREC0937) in conformity with accepted international standards following the Declaration of Helsinki. The use of human brain tissue for this project was approved by the University of Wollongong Human Research Ethics Committee (HE10/327). Approximately 1 g of frozen human occipital cortex from a neurologically normal male (81 years of age, post-mortem delay 3 h) was received from the Sydney Brain Bank (Project # PID0154). The frozen brain tissue was pulverized on dry ice and aliquots of approximately 10 mg were accurately weighed and stored at −80 °C prior to analysis. Each protocol included three replicates ($n = 3$).

Additional validation of the lipid extraction protocol was undertaken using frozen human anterior cingulate cortex from three neurologically normal males. Ages were 60, 78 and 88 years with post-mortem delay of 25, 6.5 and 9 h respectively.

Lipid Extraction

A comparison of the two lipid extraction methods is shown in Fig. 1 and each is described in detail below.

Traditional Glass-Chloroform

This protocol was based on the traditional Folch extraction [13] with modifications previously described (see [3, 27, 28]). Each 10-mg pulverized brain aliquot was homogenized on ice with a glass–glass homogenizer (1 mL Tenbroeck Tissue Grinder; Edwards Instrument Company, Narellan, NSW, Australia) in 500 μL methanol containing internal standards (plus 166 μL methanol to rinse homogenizer). The homogenate was transferred to a 4-mL vial and 1,332 μL chloroform added (chloroform/methanol 1:2, by vol). The homogenate was split, with 1/3 transferred to a

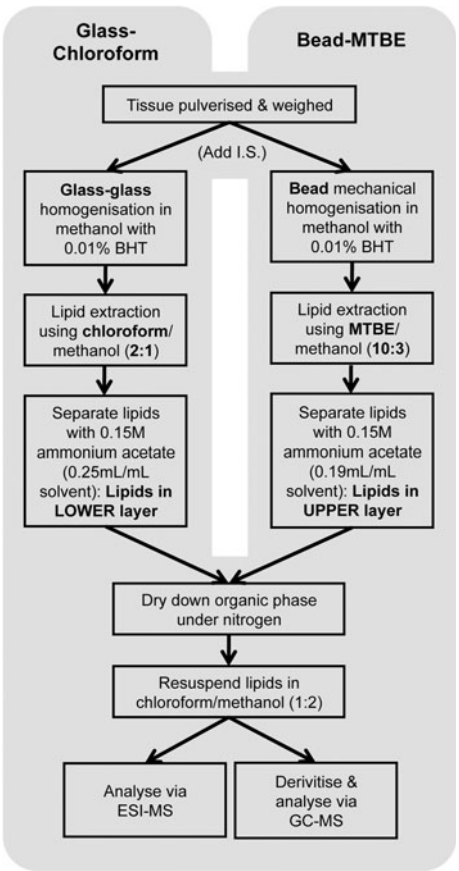

Fig. 1 Flowchart comparing lipid extraction methods: "Glass-Chloroform" versus "Bead-MTBE"; (*I.S.* internal standards; *MTBE* methyl-*tert*-butyl ether, *BHT* butylated hydroxytoluene, *ESI–MS* electrospray ionization mass spectrometry, *GC–MS* gas chromatography-mass spectrometry)

separate 4-mL vial (for phospholipid analysis), while the remaining 2/3 was used for sphingolipid and sterol analysis. Both fractions were treated equally except for the addition of sodium hydroxide (final concentration 0.7 M) to the sphingolipid and sterol fraction (to promote hydrolysis of phospholipid ester linkages). Following overnight rotation at 4 °C, 0.15 M ammonium acetate was added (chloroform/methanol/0.15 M ammonium acetate 8:4:3, by vol; 333 μL for sphingolipid/sterols and 167 μL for phospholipids), the sample centrifuged (10 min at 2,000×*g* at 4 °C) and the chloroform phase (lower phase) containing lipids transferred to a new 4-mL vial. Chloroform/methanol (1:2, by vol) was added to the original homogenate (equivalent to original volume), centrifuged as above and the lower phase combined with the first chloroform extract. A second phase separation was performed on this chloroform extract by adding 0.15 M ammonium acetate (333 μL for sphingolipid/sterols and 167 μL for phospholipids), centrifuging as above and transferring the lower phase to a new 4-mL vial (1.8-mL vial for phospholipid fraction), which was then dried under nitrogen at 37 °C. The phospholipid fraction was resuspended in 300 μL chloroform/methanol (1:2, by vol). The volume for the sphingolipid and sterol fraction was 700 μL, with half (350 μL) transferred to a 1.8-mL vial for sphingolipid analysis and the remainder (350 μL) used for sterol analysis (see below for derivatization procedures). All phospholipid and sphingolipid extracts were stored at −80 °C prior to analysis via ESI–MS.

Bead-MTBE

The MTBE extraction was modified from [20] with Precellys®24 settings based on previous work [16]. Each 10-mg pulverized brain aliquot was weighed directly into a 0.5-mL Precellys tube (Sapphire Bioscience, Waterloo, NSW, Australia) and homogenized in 300 μL ice-cold methanol containing internal standards, using a Precellys®24 (Bertin Technologies; 2 × 30 s at 6,000 rpm). After transferring the homogenate to a 4 mL glass vial the Precellys tube was rinsed with 162 μL methanol and 1,540 μL MTBE added to the glass vial (MTBE/methanol 10:3, by vol). The homogenate was split into phospholipids and sphingolipid/sterol fractions as described above. Following overnight extraction/hydrolysis, 0.15 M ammonium acetate was added (MTBE/methanol/0.15 M ammonium acetate 20:6:5, by vol; 253 μL for sphingolipid/sterols and 127 μL for phospholipids), the sample centrifuged (as above) and the organic phase (upper phase) collected in a 4-mL vial. The original homogenate was re-extracted by addition to the upper phase of MTBE/methanol/0.15 M ammonium acetate (20:6:5, by vol; 205 μL for sphingolipid/sterols and 411 μL for phospholipids), followed by centrifugation and combining the upper phase with the first extract. This lipid extract was then dried under nitrogen at 37 °C and resuspended in chloroform/methanol (1:2, by vol) as described above.

Mass Spectrometry and Lipid Analysis Settings

Phospholipid and sphingolipid extracts were analyzed via ESI–MS using a hybrid triple quadrupole ion trap mass spectrometer (QTRAP® 5500, AB SCIEX, Framingham, Massachusetts, USA) and an attached chip-based, automated nanospray source (Triversa Nanomate®, Advion, Ithaca, NY, USA). See Table 1 for ESI–MS settings. Prior to introduction on the mass spectrometer lipid extracts were diluted 1/50 with chloroform/methanol (1:2, by vol) and ammonium acetate was added (final concentration 5 μM). Samples (50 μL) were loaded onto a 96-well plate, sealed with foil and centrifuged for 10 min at 2,204×*g* (Eppendorf Centrifuge 5430). The spray parameters were set with a gas pressure of 0.4 psi and voltage applied at 1.2 and 1.1 kV for positive and negative mode respectively. Multi-channel acquisition (MCA) was employed for sphingomyelin and ceramide precursor ion scans only.

Phospholipid and sphingolipid species were quantified using AB SCIEX Lipidview™ Software (Framingham, Massachusetts, USA; see [29]). The processing settings for Lipidview™ were: mass tolerance 0.5 and minimum % intensity 0 (all species) and minimum S/N 50 (Cer, CerPCo, ChoGpl, EtnGpl) or 0 (PtdSer). Head group scans were used to quantify each lipid species (see Table 1) and the fatty acyl chain scans were used to determine each molecular species (for phospholipids only). Masses that could be assigned to ether or odd-chain fatty acids were assumed to be ether-linked phospholipids. Where two or more isomeric species from the same class were detected the relative proportion of the peak areas from each fatty acyl scan was used to calculate the final corrected areas for each molecular species. For example, ChoPCo (16:0/18:1) and ChoPCo (18:0/16:1) made up 95 and 5 % of total ChoPCo 34:1 peak areas respectively. Any species <0.5 % of lipid class were removed from the analysis. Ether-linked EtnGpl do not produce the neutral loss of 141 Da to the same extent as diacyl EtnGpl [30] and previous work in our group has demonstrated that plasmalogens produce the 141 NL at about 29 % the efficiency of diacyl EtnGpl [31]. As a diacyl internal standard was used to quantify all EtnGpl in the present study, an experimentally determined correction factor of 3.45 was applied to the ether-linked EtnGpl data (T. Mitchell, unpublished data). For ceramide the characteristic ions were $[M+H]^+$ and $[M-H_2O]^+$ for each species. The peak areas for both ions were exported from Lipidview™, combined and corrected against the combined peak areas from the internal standard.

Table 1 ESI-MS settings for phospholipid and sphingolipid analysis of human brain occipital cortex

Lipid	Ion mode	Scan type	DP	EP	CE	CXP	Range
Head group scans							
Cer	+ve	PI 264.4 *m/z*	120	14	35	10	400–700
CerPCo	+ve	PI 184.2 *m/z*	100	12	50	15	600–900
ChoGpl	+ve	PI 184.1 *m/z*	100	10	47	8	450–880
EtnGpl	+ve	NL 141 Da	100	10	30	8	420–830
PtdSer	+ve	NL 185 Da	100	10	30	8	650–830
Fatty acyl chain scans							
14:0	−ve	PI 227.2 *m/z*	−100	−10	−55	−11	400–900
16:1	−ve	PI 253.2 *m/z*	−100	−10	−55	−11	600–900
16:0	−ve	PI 255.2 *m/z*	−100	−10	−55	−11	400–900
17:0	−ve	PI 269.3 *m/z*	−100	−10	−55	−11	560–900
18:3	−ve	PI 277.2 *m/z*	−100	−10	−55	−11	600–900
18:2	−ve	PI 279.2 *m/z*	−100	−10	−55	−11	600–900
18:1	−ve	PI 281.3 *m/z*	−100	−10	−55	−11	600–900
18:0	−ve	PI 283.3 *m/z*	−100	−10	−55	−11	600–900
19:0	−ve	PI 297.3 *m/z*	−100	−10	−55	−11	600–900
20:5	−ve	PI 301.2 *m/z*	−100	−10	−55	−11	500–900
20:4	−ve	PI 303.2 *m/z*	−100	−10	−55	−11	600–900
20:3	−ve	PI 305.2 *m/z*	−100	−10	−55	−11	600–900
20:2	−ve	PI 307.2 *m/z*	−100	−10	−55	−11	600–900
20:1	−ve	PI 309.2 *m/z*	−100	−10	−55	−11	600–900
22:6	−ve	PI 327.2 *m/z*	−100	−10	−55	−11	740–900
22:5	−ve	PI 329.2 *m/z*	−100	−10	−55	−11	740–900
22:4	−ve	PI 331.2 *m/z*	−100	−10	−55	−11	740–900
22:3	−ve	PI 333.3 *m/z*	−100	−10	−55	−11	600–900

The scan rate was set at 200 Da/s for all scan types. *PI* Precursor ion, *NL* neutral loss, *DP* declustering potential, *EP* entrance potential, *CE* collision energy, *CXP* collision cell exit potential

Sterol Derivatization and GC–MS Settings

The sterol fraction of the lipid extract (from both protocols) was dried down under nitrogen at 37 °C and the following added: 1.5 mL 0.1 M hydrochloric acid, 1.5 mL 80 mM acetic acid, 250 μL 1 M sodium hydroxide and 250 μL methanol (pH of final solution ~4.75). Solid phase extraction columns (Waters Oasis Max 3 cc; Waters, Rydalmere, NSW, Australia) were preconditioned with 2 mL methanol and 2 mL 40 mM acetate buffer (pH 4.5). The sample was then loaded and washed with 2 mL 30 % methanol 40 mM formic acid (pH 4.5). Sterol fractions were eluted with 1.8 mL hexane followed by 1.8 mL acetone/hexane (30:70, by vol) and then dried down under nitrogen at 37 °C. Samples were then derivatized by the addition of 20 μL acetonitrile and 20 μL Selectra-SIL BSTFA(*N*,*O*-bis(trimethylsilyl)trifluoroacetamide) containing 1 % TMCS (trimethylchlorosilane; United Chemical Technologies, purchased from PM Separations, QLD, Australia) and incubation for 1 h at 37 °C.

After drying under nitrogen at 37 °C and reconstitution in 30 μL toluene, derivatized samples were analyzed by an Agilent 7000B triple quadrupole mass selective detector interfaced with an Agilent 7890A GC system gas chromatograph, equipped with an automatic sampler and a computer workstation. The injection port and GC–MS interface were kept at 280 °C. Separations were carried out on a fused silica capillary column (30 m × 0.2 mm i.d.) coated with cross-linked 5 % phenylmethylsiloxane (film thickness 0.33 μM; Agilent, J and W). Helium was the carrier gas with a flow rate of 1.2 mL/min (average velocity = 59 cm/sec). Derivatized samples (1 μL) were injected splitless into the GC injection port. Column temperature was increased from 165 to 270 °C at 30 °C/min after 1 min at 165 °C, then temperature was raised to 300 °C at 5 °C/min and held at 300 °C for 4 min. Selected-reaction monitoring was performed using the PCI mode using methane as the reagent gas (4 mL/min), Argon as the collision gas (1.5 mL/min) and 2.25 mL/min atomic He in the collision cell to reduce chemical noise from metastable

Table 2 Target ion transitions used for GC–MS analysis of sterols in human brain occipital cortex

Compound	Target ion transition m/z → m/z (Collision energy)
Squalene	327 → 203 (5)
(H)14-Demethyl-lanosterol	475 → 399 (6)
14-Demethyl-lanosterol	469 → 393 (4)
(H) Desmosterol	461 → 371 (10)
Desmosterol	455 → 365 (8)
(H) Campesterol	474 → 384 (8)
Campesterol	471 → 381 (8)
24,25-Dihydrolanosterol	500 → 395 (10)
Stigmasterol	395 → 255 (5)
(H) β-Sitosterol	478 → 75 (30)
β-Sitosterol	471 → 75 (25)
Lanosterol	483 → 393 (3)
(H) 24-Hydroxycholesterol	462 → 372 (8)
24-Hydroxycholesterol	455 → 365 (3)
(H) 7-Ketocholesterol	480 → 390 (20)
7-Ketocholesterol	473 → 383 (10)
(H) 27-Hydroxycholesterol	462 → 161 (15)
27-Hydroxycholesterol	457 → 161 (20)

He. The ion source was maintained at 280 °C and the quadrapoles at 150 °C. Table 2 lists the target ion transitions that were monitored for each sterol species.

Statistical Analysis

Statistical analysis was performed using JMP 9.0 (SAS Institute Inc., NC, USA). All results are expressed as means ± SEM. with $p < 0.05$ set as the level of significance. Data was tested for normality using Shapiro–Wilk W test and homogeneity of variance using a 2-sided F Test. Student's t tests were used for comparisons between treatments (Bead-MTBE versus Glass-Chloroform) for each lipid species.

Results and Discussion

Data resulting from the quantification of human occipital cortex lipids that were solvent-extracted using either the Glass-Chloroform or Bead-MTBE methods are presented in a similar format in all figures. The results for the sphingolipids, Cer and CerPCho, are shown in Figs. 2 and 3 respectively. The glycerophospholipids, ChoGpl, EtnGpl and PtdSer, are shown in Figs. 4, 5 and 6 respectively. In each of these figures, representative head group spectra from the Bead-MTBE extraction are found in the top panel (a) and the Glass-Chloroform in the middle panel (b). Comparison of these representative spectra for each lipid class reveals no obvious difference between the two methods, in terms of ions present or the maximum ion intensity (see Figs. 2, 3, 4, 5, 6; "a" vs. "b"). This indicates that the recovery levels were similar for both methods.

The lower panels (c) in Figs. 2, 3, 4, 5,and 6 show the quantified concentrations for each lipid class (nmol/g tissue wet weight). The most abundant lipid species in the human occipital cortex was ChoGpl (total ~19,000 nmol/g tissue), followed by EtnGpl (~8,000 nmol/g tissue) and PtdSer (~6,000 nmol/g tissue), CerPCho (~4,000 nmol/g tissue), with much lower levels of ceramide present (~600 nmol/g tissue). No significant difference between Bead-MTBE and Glass-Chloroform methods was evident for the total levels of each lipid class ($p > 0.28$).

Looking in more detail firstly at the sphingolipids, we identified 13 ceramide species using both extraction methods (Fig. 2c). The most abundant species were Cer(d18:1/18:0) and Cer(d18:1/24:1). Only Cer(d18:1/18:0) showed a significant increase (15 %) in concentration in the Bead-MTBE extraction ($p = 0.027$). For sphingomyelin, 15 species were identified (Fig. 3c). The major species present were: CerPCho(d18:1/18:0), CerPCho(d18:1/24:1) and CerPCho(d18:1/20:0). No significant difference between extraction protocols was evident in the level of any CerPCho species ($p > 0.14$).

In terms of the glycerophospholipids, 22 ChoGpl species were present in the human occipital cortex (20 diacyl and 2 ether), with ChoGpl(16:0/18:1) and ChoGpl(16:0/16:0) the most abundant species (Fig. 4c). No difference between the two methods was observed for ChoGpl analysis ($p > 0.11$). A total of 33 EtnGpl species were identified (18 diacyl and 15 ether species), with EtnGpl(18:0/22:6) by far the most abundant species present (Fig. 5c). Only EtnGpl(O-16:1/22:5) and EtnGpl(O-18:2/20:4) showed a significant increase (27 % each) using the Bead-MTBE extraction method ($p = 0.022$ for both). Ether-linked EtnGpl species were present at 35 % of total EtnGpl in human occipital cortex. This value corresponds with the plasmalogen levels present in normal human brains in previous studies, with values varying from 23 % in human anterior cingulate cortex and primary visual cortex [3], up to 56 % of total EtnGpl in temporal cortex grey matter [32].

No significant difference between the two protocols was observed for the PtdSer analysis ($p > 0.38$; Fig. 6c). Of the 17 PtdSer species quantified, PtdSer(18:0/18:1) and PtdSer(18:0/22:6) were present at the highest levels. Results for the lysoglycerophospholipids were consistent with their diacyl counterparts, with 12 species of lyso-ChoGpl and 10 species of lyso-EtnGpl quantified (results not shown). No significant difference between extraction methods was

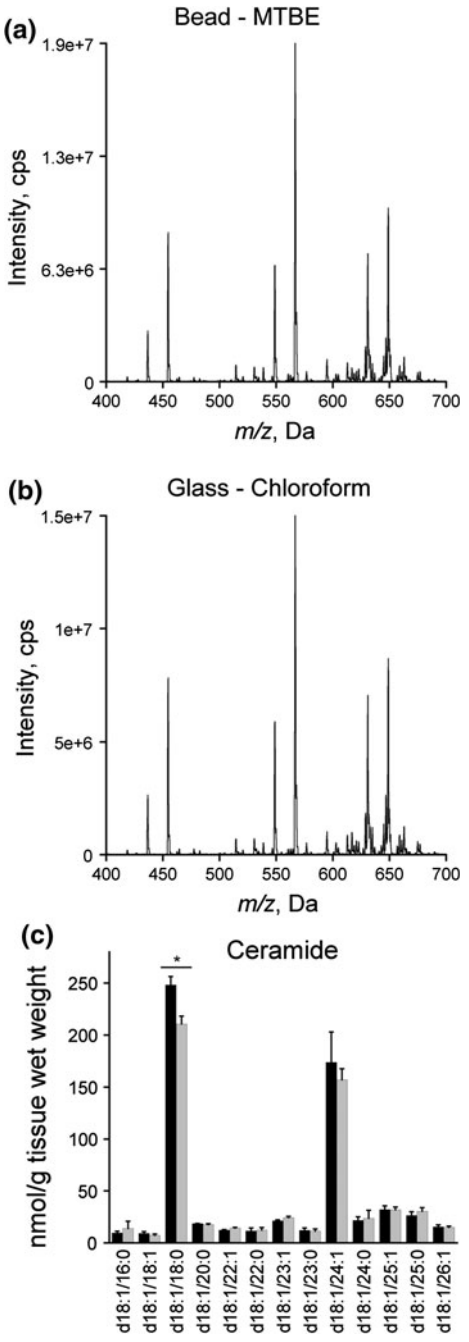

Fig. 2 Comparison of ceramide species identified in human occipital cortex using either the Bead-MTBE or Glass-Chloroform method. ESI–MS precursor ion scan targeting 264 *m/z* for: **a** Bead-MTBE extraction; **b** Glass-Chloroform extraction; **c** Quantification of brain ceramide species using both methods (Bead-MTBE *black bars*; Glass-Chloroform *grey bars*); $n = 3$ per group; *error bars* show ± SEM. $^{*}p < 0.05$

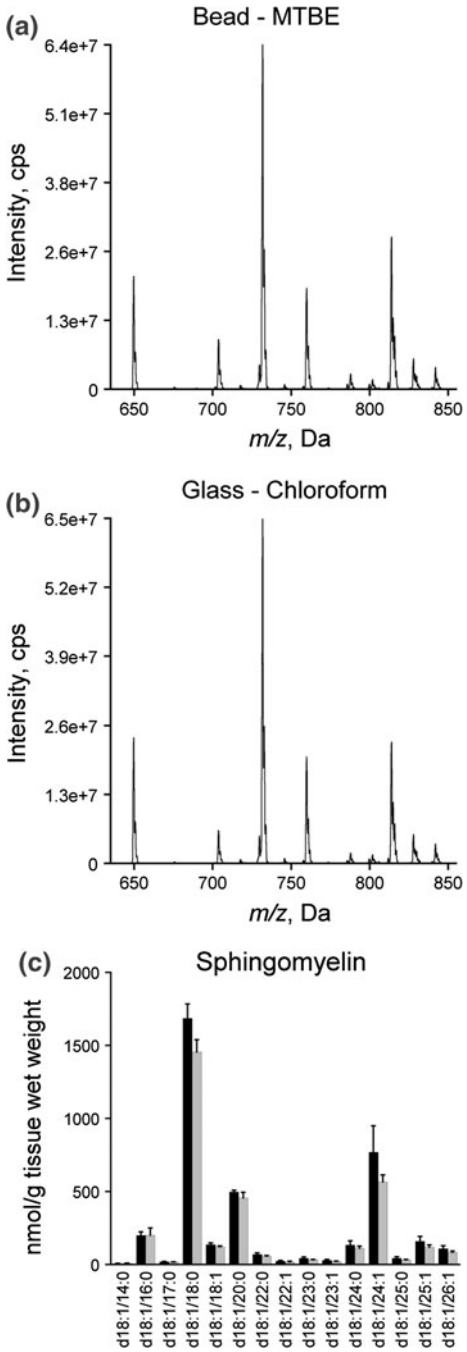

Fig. 3 Comparison of sphingomyelin (CerPCho) species identified in human occipital cortex using either the Bead-MTBE or Glass-Chloroform method. ESI–MS precursor ion scan targeting 184 *m/z* for: **a** Bead-MTBE extraction; **b** Glass-Chloroform extraction; **c** Quantification of brain sphingomyelin species using both methods (Bead-MTBE *black bars*; Glass-Chloroform *grey bars*); $n = 3$ per group; *error bars* show ± SEM

found for lyso-ChoGpl ($p > 0.11$) or lyso-EtnGpl ($p > 0.09$).

Both extraction protocols were also employed in the quantification of sterol species in the human occipital cortex (Fig. 7). Representative spectra are not shown as the quantified values were obtained using targeted multiple reaction monitoring (MRM). No significant differences were found for any sterol species when the Bead-MTBE and Glass-Chloroform extraction methods were compared (Fig. 7). The

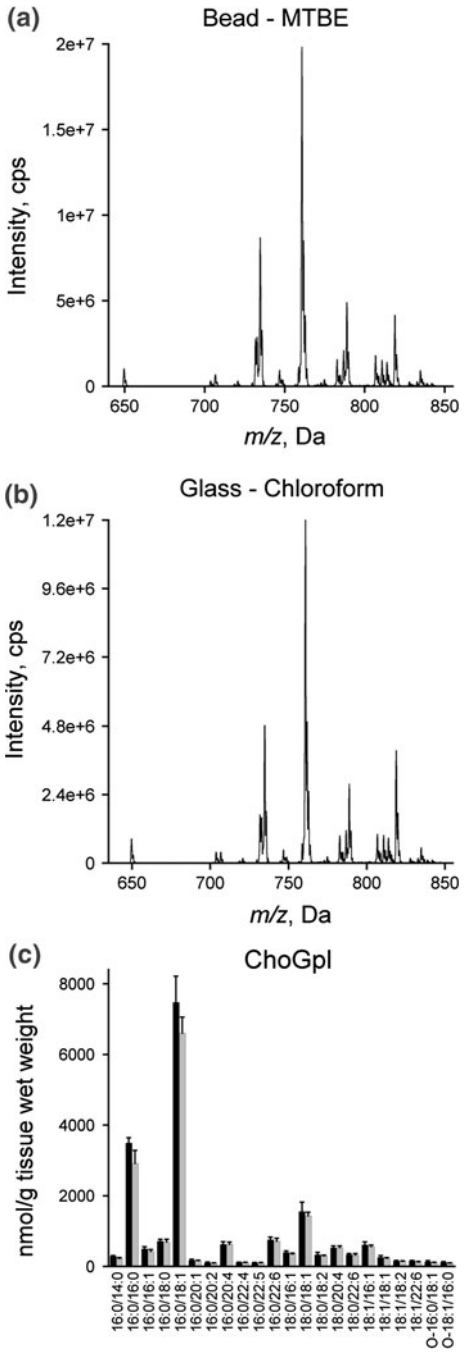

Fig. 4 Comparison of choline glycerophospholipid (ChoGpl) species identified in human occipital cortex using either the Bead-MTBE or Glass-Chloroform method. ESI–MS precursor ion scan targeting 184 *m/z* for: **a** Bead-MTBE extraction; **b** Glass-Chloroform extraction; **c** Quantification of brain choline glycerophospholipid species using both methods (Bead-MTBE *black bars*; Glass-Chloroform *grey bars*); $\underline{n} = 3$ per group; *error bars* show ± SEM

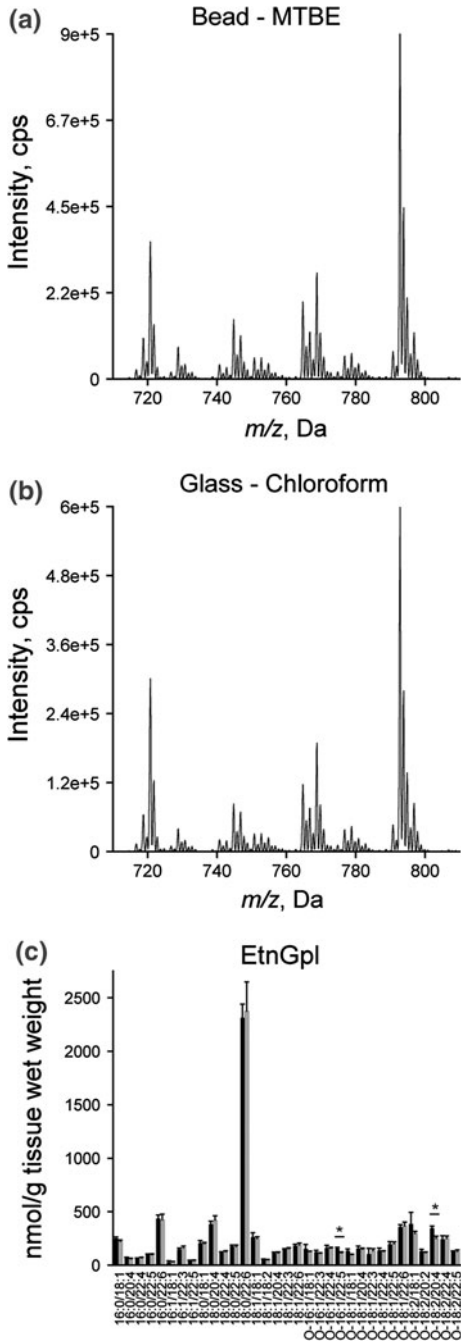

Fig. 5 Comparison of ethanolamine glycerophospholipid (EtnGpl) species identified in human occipital cortex using either the Bead-MTBE or Glass-Chloroform method. ESI–MS neutral loss scan targeting 141 Da for: **a** Bead-MTBE extraction; **b** Glass-Chloroform extraction; **c** Quantification of brain ethanolamine glycerophospholipid species using both methods (Bead-MTBE *black bars*; Glass-Chloroform *grey bars*); $n = 3$ per group; error bars show ± SEM. *$p < 0.05$

sterol species identified included cholesterol precursors (squalene, lanosterol, 14-demethyl lanosterol, desmosterol and 24,25-dihydrolanosterol), oxysterols (7-ketocholesterol, 27-hydroxycholesterol and 24-hydroxycholesterol) and phytosterols (campesterol, stigmasterol and β-sitosterol). Of the species identified, 24-hydroxycholesterol was the most highly abundant sterol species present in the human occipital cortex which is consistent with previous data [3]. As an additional measure, total free cholesterol was quantified using

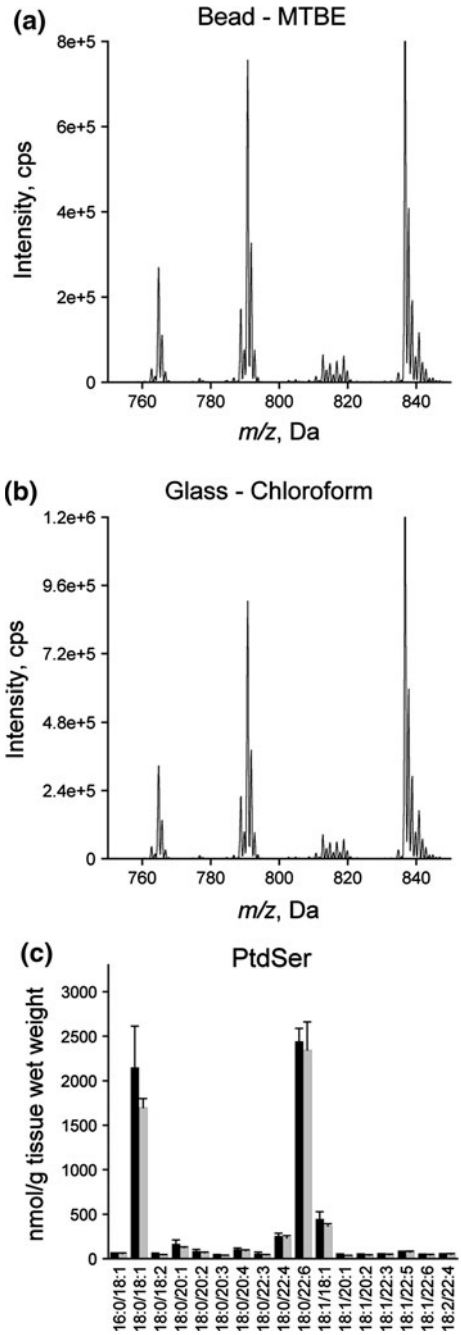

Fig. 6 Comparison of phosphatidylserine (PtdSer) species identified in human occipital cortex using either the Bead-MTBE or Glass-Chloroform method. ESI–MS neutral loss scan targeting 185 Da for: **a** Bead-MTBE extraction; **b** Glass-Chloroform extraction; **c** Quantification of brain phosphatidylserine species using both methods (Bead-MTBE *black bars*; Glass-Chloroform *grey bars*); $n = 3$ per group; *error bars* show ± SEM

ESI–MS (with lathosterol-d4 as an internal standard). In the occipital cortex cholesterol mean values were 411 ng/mg wet tissue weight (results not shown). No significant difference in cholesterol levels between the two protocols was detected ($p = 0.6842$).

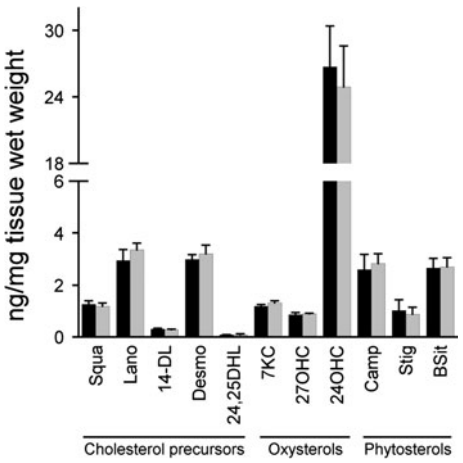

Fig. 7 Comparison of sterol species identified in human occipital cortex using either the Bead-MTBE or Glass-Chloroform method. Includes quantification of cholesterol precursors: squalene (Squa), lanosterol (Lano), 14-demethyl-lanosterol (14-DL), desmosterol (Desmo), 24,25-dihydrolanosterol (24,25DHL); oxysterols: 7-keto-cholesterol (7KC), 27-hydroxycholesterol (27OHC), 24-hydroxycholesterol (24OHC); and phytosterols: campesterol (Camp), stigmasterol (Stig) and β-sitosterol (βSit); Bead-MTBE *black bars*; Glass-Chloroform *grey bars*; $n = 3$ per group; *error bars* show ± SEM

To further validate the Bead-MTBE extraction method, we compared the sphingolipid composition of three different control subjects from a different brain region (anterior cingulate cortex). Sphingomyelin and ceramide levels in human anterior cingulate cortex are shown in Fig. 8. The sphingolipid species identified were the same as for occipital cortex (see Figs. 2, 3). For sphingomyelin, only CerPCho(d18:1/18:1) showed a significant increase in concentration in the Bead-MTBE extraction ($p = 0.033$). Three ceramide species demonstrated a significant difference between the two protocols, including Cer(d18:1/16:0), Cer(d18:1/22:1) and Cer(d18:1/23:1), with p values of 0.034, 0.001 and 0.017 respectively. The sphingolipid species with significant differences between the two protocols were all low abundance species. These results are comparable to the single occipital cortex sample and demonstrate that there are no major differences between the two methods when samples from multiple donors are analyzed.

From these studies we conclude that the high-throughput Bead-MTBE protocol is equivalent to the traditional Glass-Chloroform protocol for lipid extraction and quantification of glycerophospholipid, sphingolipid and sterol species in human brain tissue. Furthermore, the average variation for each lipid class was also similar, with the following coefficient of variation (CV) values for Bead-MTBE and Glass-Chloroform respectively: Cer, 20.1 and 23.3 %; CerPCho, 25.3 and 17.0 %; ChoGpl, 21.9 and 15.0 %; EtnGpl, 21.4 and 13.1 %; PtdSer, 24.7 and 15.2 %; and sterols, 22.4 and

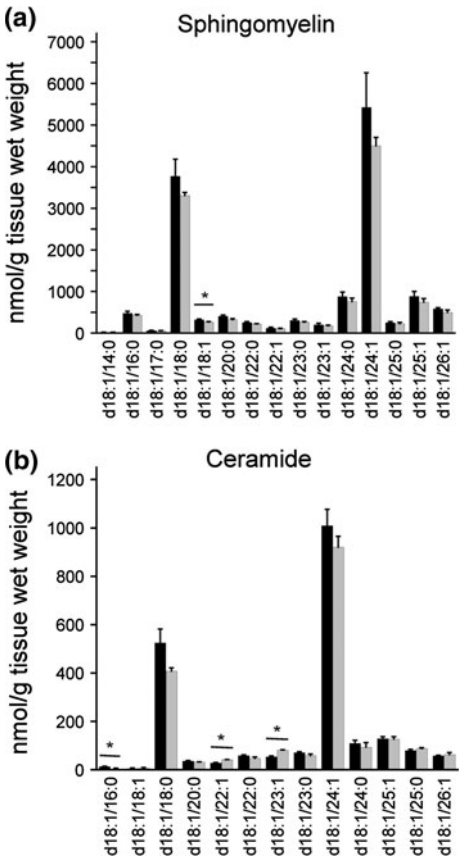

Fig. 8 Quantification of human anterior cingulate cortex sphingolipid species; **a** sphingomyelin; **b** ceramide species using both extraction methods (Bead-MTBE *black bars*; Glass-Chloroform *grey bars*); $n = 3$ different control subjects per group; *error bars* show ± SEM. $^*p < 0.05$

23.5 %. The data suggest that the Bead-MTBE method may be slightly more efficient than the traditional Folch extraction using glass–glass homogenizers for lipid extraction. From Figs. 2, 3, 4, 5,and 6 it is obvious that there is a trend for increased levels of lipids detected using the Bead-MTBE extraction relative to Glass-Chloroform extraction, with a significant increase in a small number of lipid molecular species for Bead-MTBE (Cer and EtnGpl only). This indicates that lipid recoveries using this new extraction method may be improved slightly.

As mentioned above, we observed significant increases in three lipid species with the Bead-MTBE extraction in the present study ($p < 0.05$). It should be noted, however, that of the total 133 lipid species identified we would expect to find a significant difference for 5 % of these species by chance alone (i.e. 6 or 7 species). Therefore, with significant differences for only three lipid species, we can safely conclude that there was no difference in lipid composition results when Bead-MTBE and Glass-Chloroform extraction methods were compared.

We based the MTBE extraction method used in the present study on our own modified Folch protocol (see [27, 28]), as opposed to the variation of Folch used in [20]. That is, we used 0.15 M ammonium acetate instead of water for phase separation, as the use of a salt should increase the partition coefficient and reduce the loss of lipids in the aqueous phase [13]. Although brain samples were homogenized in methanol in the current protocol, we also tested homogenization in 0.01 % w/v ammonium acetate, followed by extraction with MTBE/methanol (as per [20]; results not shown). Results were similar to the sphingolipid and glycerophospholipid classes quantified using Bead-MTBE and Glass-Chloroform, indicating that homogenization of brain tissue in methanol or 0.01 % ammonium acetate is equivalent.

Based on the knowledge that sulfatides are known to be enriched in the brain [33], we also determined the mol % distribution of sulfatide species in human occipital cortex (data not shown). A total of 18 sulfatide species were identified. Only two minor species (SGalCer 41:2;2 and SGalCer 42:3;2) demonstrated a significant increase in the Bead-MTBE extraction protocol, indicating that sulfatide brain levels can be accurately determined using the Bead-MTBE lipid extraction method.

In addition to the comparison between the Bead–MTBE and Glass–Chloroform extraction methods, we also tested the influence of increasing brain tissue amounts on the extraction efficiency of MTBE/methanol for the various lipid classes (results not shown). Total solvent volume remained constant (~2 mL) while increasing the amount of control tissue to be extracted (i.e. 10, 20 and 40 mg). On average the variation between tissue amounts was ≤10 % for all quantified glycerophospholipids (including ChoGpl, EtnGpl and PtdSer), as well as CerPCho. The average variation for ceramide was higher (31 %), with significantly reduced quantitation levels at 20 and 40 mg tissue mass. The mol % values for ceramide species within ceramide class appeared to be consistent, however, indicating that the relative species distribution is maintained for up to 40 mg of tissue. This apparent lower recovery of ceramide species at higher tissue:solvent ratios may be to due the much lower abundance of this lipid class (for example, ChoGpl is present at 33 times the levels of Cer in the occipital cortex). Therefore, although 2 mL MTBE/methanol is sufficient for the quantification of glycerophospholipids and sphingomyelin in up to 40 mg brain tissue, if ceramide is to be included in the analysis we would recommend increasing solvent volumes accordingly to avoid under-estimation of this lipid class.

In summary, lipid profiling of human brain using MTBE extraction and mechanical bead homogenization was comparable to Folch extraction (i.e. chloroform) with glass–glass homogenization. This was true for sphingolipids (ceramide and sphingomyelin), glycerophospholipids (choline glycerophospholipids, ethanolamine glycerophospholipids and

phosphatidylserine) and sterols. This high-throughput Bead-MTBE protocol improves upon traditional lipid extraction methods as it is safer and much more efficient. The Bead-MTBE protocol is approximately four times quicker than Glass-Chloroform in the homogenization of 24 samples (i.e. 1 vs. 4 h), with the additional benefit being that tissue aliquots can be weighed directly into the Precellys tubes prior to homogenization (thus reducing double-handling times). The lower density of MTBE further enhances the lipid extraction procedure (by dissolving lipids in the upper phase) and is also better for the potential incorporation of robotics to further streamline lipidomic studies.

Acknowledgments Adult brain tissue was received from the Sydney Brain Bank at Neuroscience Research Australia which is supported by the National Health and Medical Research Council of Australia, the University of New South Wales and Neuroscience Research Australia. This research was supported by a project grant (APP1008307) from the Australian National Health and Medical Research Council (NHMRC) awarded to GMH and BG. TWM and BG are supported by Australian Research Council Future Fellowships (FT110100249 and FT0991986, respectively). GMH is supported by an NHMRC Principal Research Fellowship (630434).

Conflict of interest All authors disclose that there are no conflicts of interest.

References

1. Ledesma MD, Martin MG, Dotti CG (2012) Lipid changes in the aged brain: effect on synaptic function and neuronal survival. Prog Lipid Res 51:23–35
2. Conde C, Martinez M, Ballabriga A (1974) Some chemical aspects of human brain development. I. Neutral glycosphingolipids, sulfatides, and sphingomyelin. Pediatr Res 8:89–92
3. Cheng D, Jenner AM, Shui G, Cheong WF, Mitchell TW, Nealon JR, Kim WS, McCann H, Wenk MR, Halliday GM, Garner B (2011) Lipid pathway alterations in Parkinson's disease primary visual cortex. PLoS ONE 6:e17299
4. Fabelo N, Martín V, Santpere G, Marín R, Torrent L, Ferrer I, Díaz M (2011) Severe alterations in lipid composition of frontal cortex lipid rafts from Parkinson's disease and incidental Parkinson's disease. Mol Med 17:1107–1118
5. Hejazi L, Wong JWH, Cheng D, Proschogo N, Ebrahimi D, Garner B, Don AS (2011) Mass and relative elution time profiling: two-dimensional analysis of sphingolipids in Alzheimer's disease brains. Biochem J 438:165–175
6. Garner B (2010) Lipids and Alzheimer's disease. Biochim Biophys Acta Mol Cell Biol Lipids 1801:747–749
7. Karasinska JM, Hayden MR (2011) Cholesterol metabolism in Huntington disease. Nat Rev Neurol 7:561–572
8. Schwarz E, Prabakaran S, Whitfield P, Major H, Leweke FM, Koethe D, McKenna P, Bahn S (2008) High throughput lipidomic profiling of schizophrenia and bipolar disorder brain tissue reveals alterations of free fatty acids, phosphatidylcholines, and ceramides. J Proteome Res 7:4266–4277
9. Eisenstein M (2011) Genetics: finding risk factors. Nature 475:S20–S22
10. Bertram L, Tanzi RE (2012) The genetics of Alzheimer's disease. Prog Mol Biol Transl Sci 107:79–100
11. Fonteh AN, Harrington RJ, Huhmer AF, Biringer RG, Riggins JN, Harrington MG (2006) Identification of disease markers in human cerebrospinal fluid using lipidomic and proteomic methods. Dis Markers 22:39–64
12. Blanksby SJ, Mitchell TW (2010) Advances in mass spectrometry for lipidomics. Annu Rev Anal Chem 3:433–465
13. Folch J, Lees M, Sloane Stanley GH (1957) A simple method for the isolation and purification of total lipids from animal tissues. J Biol Chem 226:497–509
14. Cequier-Sánchez E, Rodríguez C, Ravelo AG, Zárate R (2008) Dichloromethane as a solvent for lipid extraction and assessment of lipid classes and fatty acids from samples of different natures. J Agric Food Chem 56:4297–4303
15. Carlson LA (1985) Extraction of lipids from human whole serum and lipoproteins and from rat liver tissue with methylene chloride-methanol: a comparison with extraction with chloroform-methanol. Clin Chim Acta 149:89–93
16. Fraser T, Tayler H, Love S (2008) Low-temperature improved-throughput method for analysis of brain fatty acids and assessment of their post-mortem stability. J Neurosci Methods 169:135–140
17. Fraser T, Tayler H, Love S (2010) Fatty acid composition of frontal, temporal and parietal neocortex in the normal human brain and in Alzheimer's disease. Neurochem Res 35:503–513
18. Römisch-Margl W, Prehn C, Bogumil R, Röhring C, Suhre K, Adamski J (2012) Procedure for tissue sample preparation and metabolite extraction for high-throughput targeted metabolomics. Metabolomics 8:133–142
19. Wu H, Southam AD, Hines A, Viant MR (2008) High-throughput tissue extraction protocol for NMR- and MS-based metabolomics. Anal Biochem 372:204–212
20. Matyash V, Liebisch G, Kurzchalia TV, Shevchenko A, Schwudke D (2008) Lipid extraction by methyl-*tert*-butyl ether for high-throughput lipidomics. J Lipid Res 49:1137–1146
21. Kosicek M, Kirsch S, Bene R, Trkanjec Z, Titlic M, Bindila L, Peter-Katalinic J, Hecimovic S (2010) Nano-HPLC–MS analysis of phospholipids in cerebrospinal fluid of Alzheimer's disease patients—a pilot study. Anal Bioanal Chem 398:2929–2937
22. Kosicek M, Zetterberg H, Andreasen N, Peter-Katalinic J, Hecimovic S (2012) Elevated cerebrospinal fluid sphingomyelin levels in prodromal Alzheimer's disease. Neurosci Lett 516:302–305
23. Bligh EG, Dyer WJ (1959) A Rapid method of total lipid extraction and purification. Can J Biochem Physiol 37:911–917
24. Graessler J, Schwudke D, Schwarz PEH, Herzog R, Shevchenko A, Bornstein SR (2009) Top-down lipidomics reveals ether lipid deficiency in blood plasma of hypertensive patients. PLoS ONE 4:e6261
25. Ki Ichihara, Yoneda K, Takahashi A, Hoshino N, Matsuda M (2011) Improved methods for the fatty acid analysis of blood lipid classes. Lipids 46:297–306
26. Schuhmann K, Almeida R, Baumert M, Herzog R, Bornstein SR, Shevchenko A (2012) Shotgun lipidomics on a LTQ Orbitrap mass spectrometer by successive switching between acquisition polarity modes. J Mass Spectrom 47:96–104
27. Deeley JM, Mitchell TW, Wei X, Korth J, Nealon JR, Blanksby SJ, Truscott RJW (2008) Human lens lipids differ markedly from those of commonly used experimental animals. Biochim Biophys Acta Mol Cell Biol Lipids 1781:288–298
28. Saville JT, Zhao Z, Willcox MDP, Blanksby SJ, Mitchell TW (2010) Detection and quantification of tear phospholipids and cholesterol in contact lens deposits: the effect of contact lens material and lens care solution. Invest Ophthalmol Visual Sci 51:2843–2851
29. Ejsing CS, Duchoslav E, Sampaio J, Simons K, Bonner R, Thiele C, Ekroos K, Shevchenko A (2006) Automated identification and

quantification of glycerophospholipid molecular species by multiple precursor ion scanning. Anal Chem 78:6202–6214
30. Zemski Berry K, Murphy R (2004) Electrospray ionization tandem mass spectrometry of glycerophosphoethanolamine plasmalogen phospholipids. J Am Soc Mass Spectrometry 15:1499–1508
31. Mitchell TW, Buffenstein R, Hulbert AJ (2007) Membrane phospholipid composition may contribute to exceptional longevity of the naked mole-rat (Heterocephalus glaber): a comparative study using shotgun lipidomics. Exp Gerontol 42:1053–1062
32. Ginsberg L, Rafique S, Xuereb JH, Rapoport SI, Gershfeld NL (1995) Disease and anatomic specificity of ethanolamine plasmalogen deficiency in Alzheimer's disease brain. Brain Res 698:223–226
33. Han X, Holtzman DM, McKeel DW, Kelley J, Morris JC (2002) Substantial sulfatide deficiency and ceramide elevation in very early Alzheimer's disease: potential role in disease pathogenesis. J Neurochem 82:809–818